STABILITY OF BURIED SCOUR PROTECTION IN SHALLOW COASTAL WATERS

Nils B. Kerpen[1], Alexander Schendel[1], Henry Forgan[2],
Dirk Jan Peters[2], Erik Zigterman[2] and Torsten Schlurmann[1]

Physical model tests were conducted to verify the stability of a conceptual scour protection design placed around monopiles in varying water depth and under combined wave and current load. The tests were performed in a 3D wave-current basin at Ludwig-Franzius-Institute, Leibniz University Hannover in a model scale of 1:35. As a unique boundary condition compared to previous studies, the scour protection around the monopile was placed below a mobile sand bed. Before waves and current could act on the scour protection, the overlaying sand layer had to be eroded. The scouring process of this sand layer was evaluated, and the stability of the armour layer of the underlying scour protection quantitatively assessed. The characteristics of the scour development and the damage of the armour layer were described as a function of several wave-current load combinations and different morphodynamic stages of the beach.

Keywords: erosion; monopile; scour depth; buried scour protection; hydraulic model test

INTRODUCTION

In view of the progressive development of offshore wind energy towards greater water depths in recent years (WindEurope, 2021), research on scour around offshore structures has mainly focused on its development under typical offshore sea states and water depths (Sumer and Fredsøe, 2002; Qi and Gao, 2014; Schendel et al., 2020). Likewise, present formulae for the design of granular scour protection (De Vos et al., 2012) are also based on these boundary conditions. To date there are no guidelines available for an accurate assessment of scour protection stability under the unique and complex conditions found in the tidal zone of a beach, where the combination of strong currents, wave breaking, and active morphological processes occur simultaneously and drive rapid changes of a shallow water bathymetry.

Thus, this novel experimental study aims to improve the understanding of scouring processes and scour protection stability around monopile support structures placed in shallow coastal waters ($0.047 < d/L_p < 0.057$). As an additional unique boundary condition compared to previous scour protection related studies, the scour protection around the monopile is installed below a mobile sand bed. The characteristics of the scour development of the upper sand layer and the deformation of the scour protection are described as a function of several wave-current load combinations, different morphodynamic stages of the beach and the outer extent of the scour protection. The stability of the scour protection is quantitatively evaluated by dimensionless damage numbers.

HYDRAULIC MODEL TESTS

Model set-up

The hydraulic model tests were performed in the 3D wave-current basin of the Ludwig-Franzius-Institute, Hannover, Germany, in a model length scale of 1:35 (FROUDE scaling, Figure 1). The basin has a length of 40 m, a width of 24 m and can be filled up to a maximum water depth of about 1 m.

The global bathymetry was built by sand covered with a sand-cement layer of about 0.1 m thickness. Walls to guide the flow and the waves into the test area were built from plywood and were supported by prefabricated concrete elements. From the wave maker a transition slope (1:10) was constructed on the horizontal concrete floor of the basin. Next to the transition slope, a horizontal foreshore (0.402 m above basin floor) was constructed of sand with a top layer of sand-cement. This horizontal foreshore section was followed by a second sloped section (1:30). At the end of this section, the monopile was located. From the position of the monopile to the passive wave absorbers at the outer edge of the wave basin, the bathymetry remains horizontal (0.485 m above basin floor). Passive foam absorbers behind the test section enabled stable boundary conditions by a significant reduction of reflections.

The current is generated by four pumps that recirculate the water in the basin below the basin floor. The current was guided into the model area over a weir that enables the control of the required discharge and thereby the current flow velocity in the test section. Behind the weir, the current was flowing towards

[1] Ludwig-Franzius-Institute for Hydraulic, Estuarine and Coastal Engineering, Leibniz University Hannover, Nienburger Str. 4, 30167 Hannover, Germany

[2] HaskoningDHV Nederland B.V., Postbus 151, 6500AD Nijmegen, Jonkerbosplein 52, 6534 AB Nijmegen, The Netherlands.

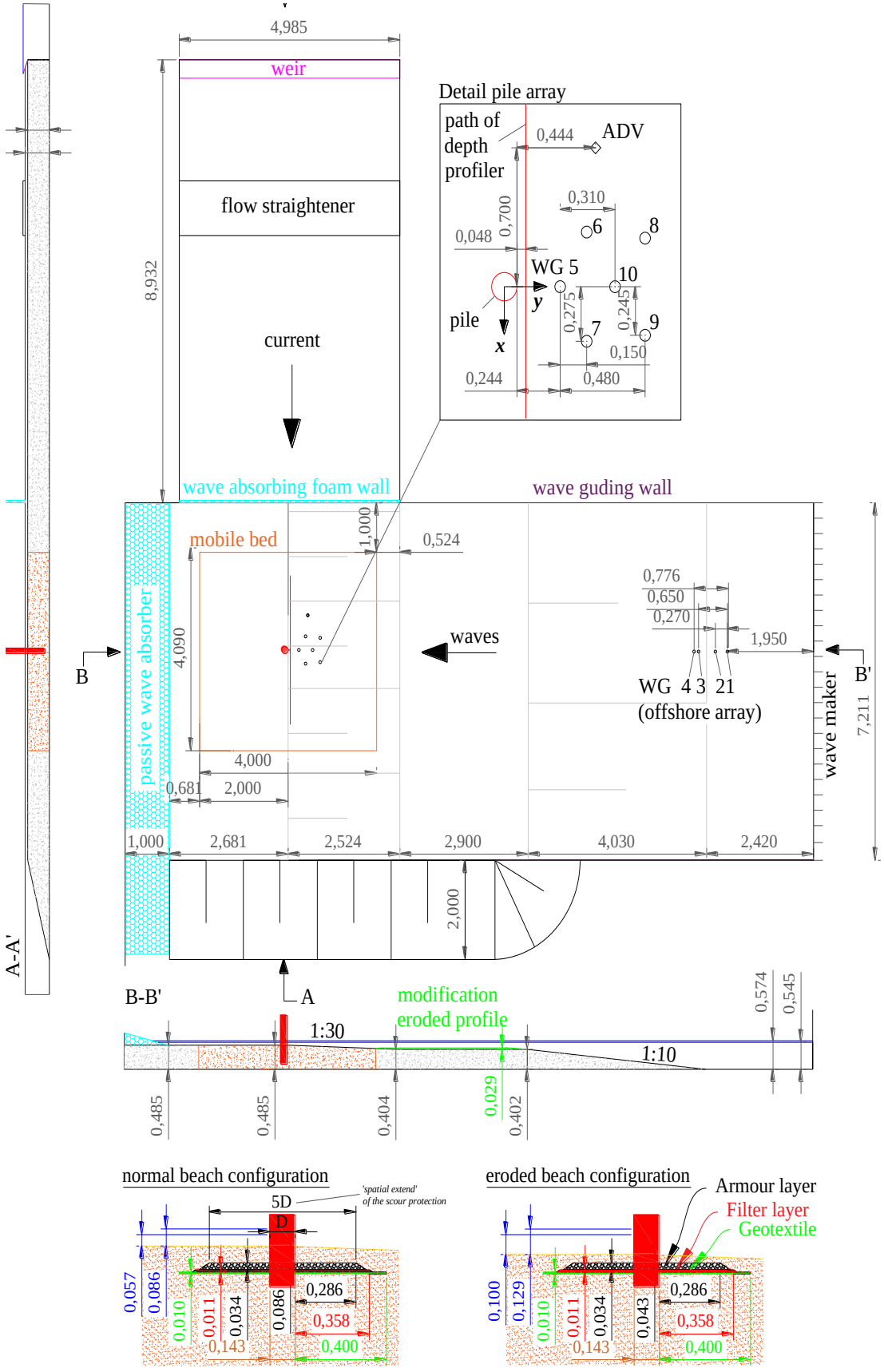

Figure 1. Model set-up in the wave basin as top-view, cross section and detail of the buried scour protection layers. Measures in meter, model scale: 1:35.

the test section via an erected side channel of about 5 m width before reaching the test section.

In the center of this set-up a 4m x 4m wide mobile bed section was installed and a monopole (diameter D = 0.14 m) was placed in the center. Wave and current conditions were measured in the near and far field of the monopile. Prototype conditions at the pile ranged as follows: Water depth 2 m < d < 4.5 m, flow velocities 0 < u_c < 2.5 m/s, wave heights 1.8 < H_{m0} < 3.8 and wave periods 8.8 s < $T_{m\text{-}1,0}$ < 9.9. Two load scenarios with return periods of 1/10 year and 1/100 year were tested. Irregular waves (JONSWAP spectra with a peak enhancement factor γ = 3.3, and spectral width parameters σ_a= 0.07 and σ_b = 0.09) were adopted for all tests. Hydraulic processes were observed by wave gauges and arrays, by 3D velocity probes, depth profilers and a number of cameras in- and outside the pile.

Rock grading for the scour protection

A three-layer scour protection setup was used, consisting of a granular armour layer on top of a granular filter layer and a geotextile. The bottom geotextile was used to replace a widely graded granular filter layer to effectively prevent winnowing and focus on shear failure of the armour layer.

The rock gradings for the filter and armour layers were selected based on the requirements and limitations of the EN 13383 system for standardizing rock grading (CIRIA, 2007) and represent idealized Rosin-Rammler distributions.

To avoid cohesive sediment behavior for finer fractions, the stone gradings were not scaled according to FROUDE similarity. Instead, the stone diameter was scaled to maintain a mobility similar to the prototype dimensions under the given hydrodynamic loads (Whitehouse, 1998; Deltares, 2016). This is achieved by scaling each fraction within a stone grading with respect to the mobility parameter similarity. The mobility parameter describes the ratio between acting and critical Shields parameter:

$$MOB = \theta_{cw} / \theta_{cr} \qquad (1)$$

with θ_{cw} as the Shields parameter due to combined wave and current load, and θ_{cr} the critical Shields parameter of the considered stone. Compared with the MOB scaling, FROUDE scaling would lead to larger maximum stone diameters, resulting in less damage and an overly optimistic stability assessment. The individual layer thicknesses as well as spatial extent are given in Figure 1.

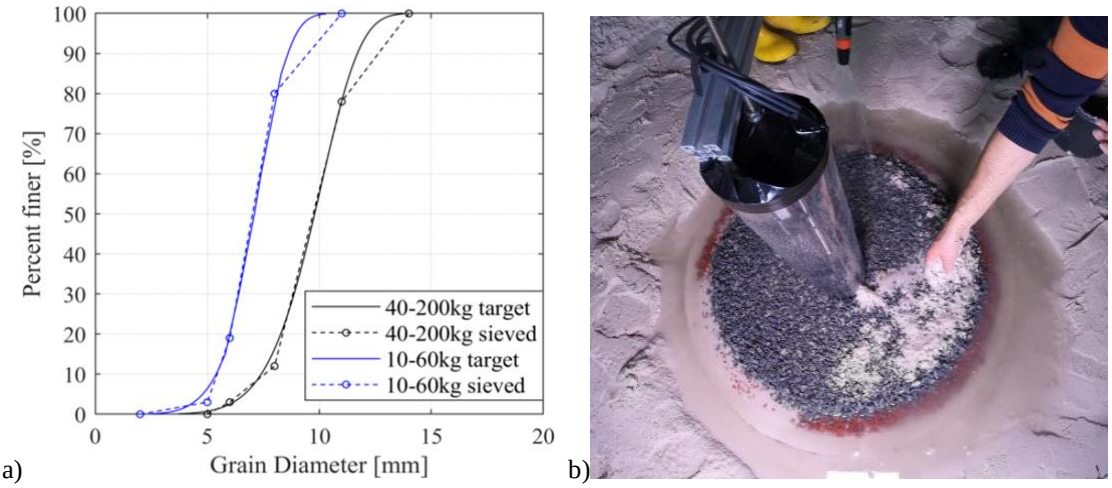

Figure 2. a) Grading of the scour protection (model scale). b) Scour protection in the installation process while sand is carefully being washed into the pores between the stones.

Test procedure

First, the scour protection was installed in the mobile bed section around the monopile (Figure 2b). The mobile test section had dimensions of 4x4x0.48 m and was filled with sand of a median grain diameter of d_{50} = 0.17 mm, a geometric standard deviation σ_g = 1.4 and a density of ρ_s = 2.65 g/cm³. The final placement of the scour protection was then documented by a 3D laser scan. In the tests simulating a "normal" beach configuration, the top of the scour protection was 8.6 cm (model dimensions) below the sand line, in the "eroded" beach configuration the burial depth was 4.3 cm. Then, the scour protection was covered with sand and the surface was levelled. The sand was carefully washed into the porous grain structure of the scour protection to reduce the amount of entrapped air. Another 3D laser scan was conducted to document the initial beach configuration. Finally, the basin was filled to the required water level.

In tests with wave load, at least 3,000 waves were applied, after which only a limited increase in damage to the scour protection is expected (Chavez et al., 2019; De Vos et al., 2012). As it was intended to keep the number of waves between tests comparable, the duration of a test increased with larger peak wave periods. The bed topography was profiled along a cross section close to the pile in regular intervals during a test. In most of the tests, the water was slowly drained from the basin after a test until the scour hole was dry. The scour hole was documented photographically and measured by a 3D laser scan (Faro Focus 3D).

In a series of tests with continuously increasing hydraulic loading, the scour hole caused by the first loading was left intact and the basin was refilled with water for the next test. At the end of a series of tests, the entire scour protection was removed and completely rebuilt for the next series of tests. An impression of the hydraulic model tests is given in Figure 3.

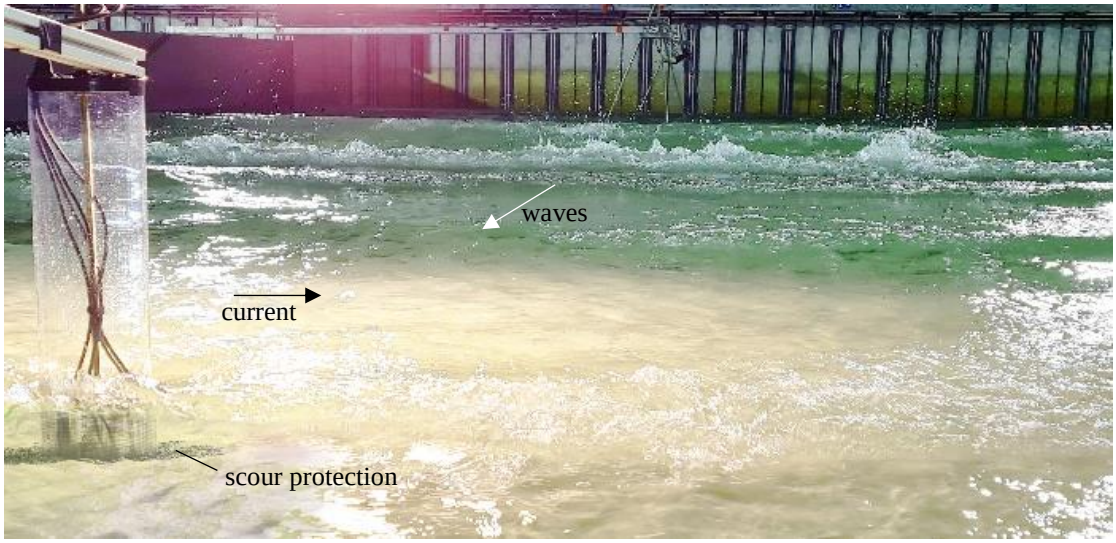

Figure 3. Impression of the Monopile in the wave basin.

RESULTS

In the following, the erosion processes and scour evolution of the sand layer above the scour protection is discussed first. Then, a stability assessment of the initially buried scour protection follows.

Scour process

Figure 4 illustrates the differences in scour patterns as a result of the three different loading scenarios: a) current only, b) wave only and c) combined wave and current conditions. In the wave-only test, the wave height was H_{m0}= 5.23 m, whereas in the current-only test, a current with a velocity of u_c = 2.25 m/s was applied.

It can be seen that the wave-only conditions were not able to erode the sand cover and that also a local scour was rarely visible. The current-only conditions on the other hand led to the formation of a distinct scour hole, the depth of which is limited by the former buried scour protection layer. It is assumed that by reaching the scour protection layer further progression and expansion of the scour hole was obstructed as the rotating horseshoe vortex could not develop to its maximum size and strength. The final shape of the scour hole evolved towards the radial, slightly asymmetrical form typical for current induced scouring process. As found by Schendel et al. (2019), the shape of the scour hole can to be more symmetrically under tidal current flow than under the unidirectional condition testing herein.

Under the combined wave-current loading, the shape and extent of the scour hole was similar to that of the current-only test despite the additional wave loading. Given the similar shape, extent and depth of the scour hole, it could be assumed that the current was thus the dominant driver of the scour development. However, as the depth and extent of the scour hole was limited by the scour protection, it is difficult to say how the scour development would have progressed in its absence.

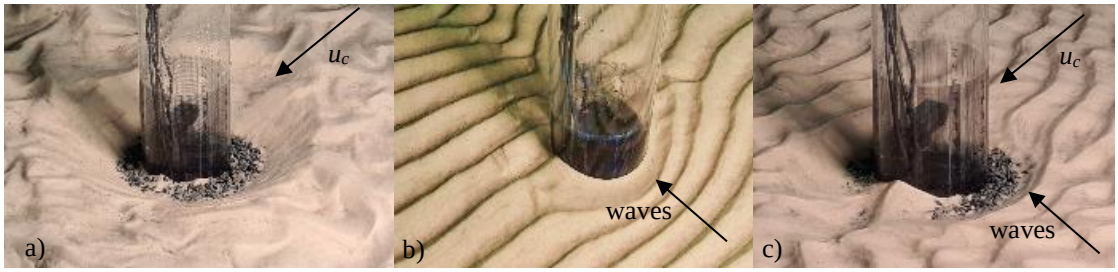

Figure 4. Scour pattern around the monopile in shallow coastal water (normal beach profile) after (a) current only-, (b) waves only- and (c) waves and current loading.

To show further differences in the shape of the scour hole, Figure 5 depicts cross-sections through the scour hole in the direction of the current for all 3 load cases. As mentioned above, a distinct scour hole is hardly visible under wave-only load. Under current load, the scour hole tended to be slightly asymmetrically, characterized by steeper slopes and a smaller extension on the upstream side of the pile (in current direction) compared to the downstream side. At the end of the current-only test, the scour hole extended to a distance of around 1.9 D from the pile in flow direction, which is slightly less than might have been expected as a final extent for a current induced scour hole (Whitehouse, 1998). With additional wave loading, the extent of the scour hole downstream of the pile reached 2.5D, slightly further than under current only conditions.

To illustrate the limiting effect of the buried scour protection on the scour process, Figure 6 compares three combined wave-current tests in which the current intensity was gradually increased from 1.75 m/s to 2.25 m/s every 4000 waves. While the size of the scour hole increased slightly and the slopes became less steep with increasing flow intensity, the scour depth was limited by the scour protection. However, a greater area of the amour layer was exposed with increasing current load.

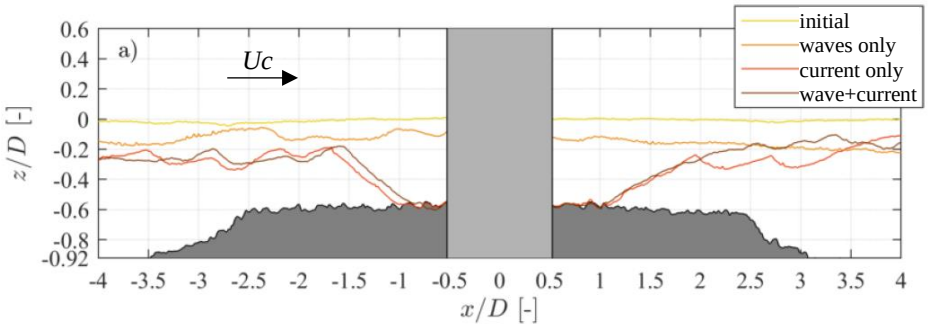

Figure 5. Erosion of the sand cover based on different load scenarios. Current from the left, Waves from the image plane towards the viewer.

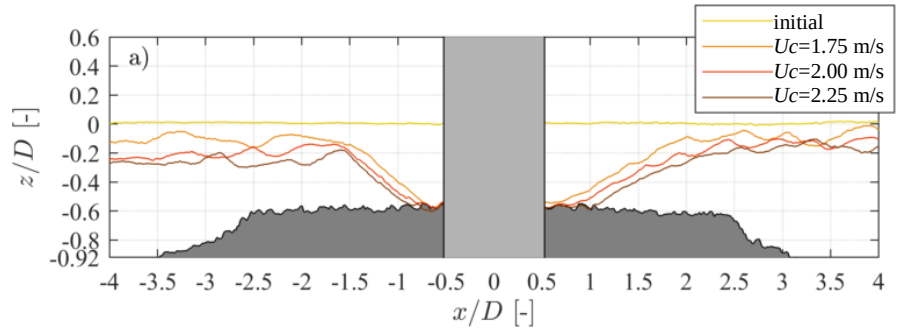

Figure 6. Subsequent progression of erosion with increasing flow velocity under combined wave and current load. The erosion conditions are the result from a sequence of increasing current loads with the simultaneous presence of waves.

For tests with an eroded beach profile, most of the scour protection was uncovered. In current and wave-current conditions, the level of stone movement reached from “rocking” of exposed stones to a clear albeit local deformation of the scour protection layer. The movement of stones increased with increasing current flow velocity, thinner sand cover and increasing water depth, which are boundary conditions inherent to the eroded beach profile.

Stability assessment of the scour protection

The deformation of the armour layer was measured using 3D laser scans and further analyzed by non-dimensional damage numbers, which provide a means to assess and compare the stability of the scour protection design. The three-dimensional damage number

$$S = \frac{V_e}{d_{n,50} A_{sub}} \quad (2)$$

introduced by De Vos et al. (2012) is defined as the ratio of the eroded volume V_e and the surface of the sub-area (A_{sub}) times the nominal median stone diameter $d_{n,50}$. The approach was inspired by the two-dimensional damage number derived by Van der Meer (1988). In contrast to De Vos et al. (2012), an area equal to $A_{sub} = 4d_{n,50}$ was selected for this study as a settling of the armour layer was only observed in close vicinity of the pile for many tests. Furthermore, this area directly corresponds to the failure criterion by den Boon et al. (2004), which considers the protective function to have failed when the filter layer is exposed over an area equal to the footprint of four armour stones $4d_{n,50}^2$. With this approach, a damage number of $S = 1$ implies that the scour protection is eroded by a thickness of $d_{n,50}$ within the considered sub-area (A_{sub}). Applying the failure criterion by den Boon et al. (2004) as reference area for the damage assessment was introduced and reviewed in Fazeres-Ferradosa et al. (2020).

The maximum damage number for the whole scour protection can be calculated from the individual damage numbers by:

$$S_{\max} = max_{i=1}^{\#sub-areas}(S_i) \quad (3)$$

The procedure of the calculation of the damage number based on differences in the bed elevation is highlighted exemplarily in Figure 7 for one selected test case.

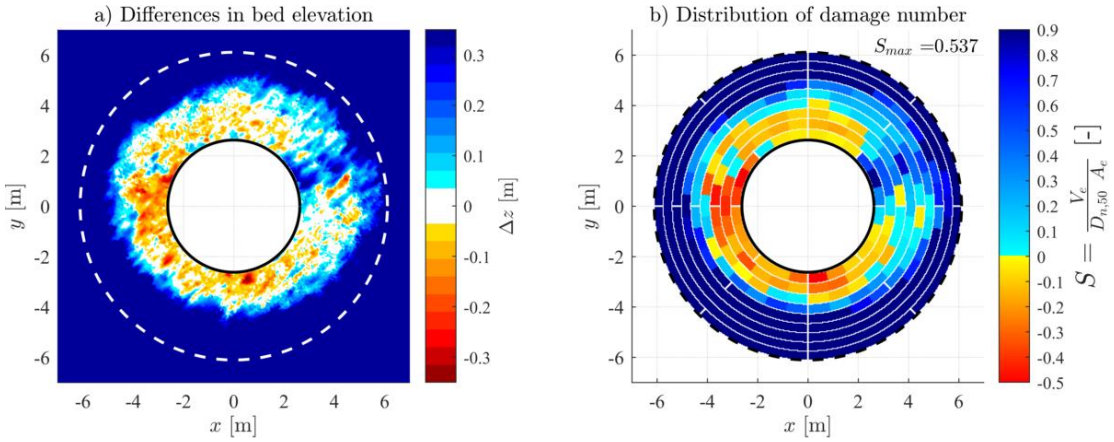

Figure 7. a) Difference in the bed elevation measured with a 3D laser scanner by subtraction of digital elevation model from before and after a test. b) Distribution of the corresponding damage number.

As both waves-only conditions (1/10 and 1/100 return interval) were incapable to uncover the scour protection from the sand layer, no damage of the armour layer was induced. Current-induced load was also not sufficient to lead to significant damage to the amour layer. However, "rocking" and movement of single exposed stones was observed during the current-only conditions. Accordingly, only small maximum damage numbers below $S_{max} = 0.19$ were determined, which occurred at the upstream side of the pile. The superposition of current with waves resulted in an increased load compared to the current-only conditions and consequently a more pronounce stone movement and armour layer deformation could be observed.

Figure 8 shows the determined damage numbers with respect to the corresponding flow velocity with and without the presence of waves for the normal and the eroded beach configuration. As expected, the damage increased with increasing flow velocity. The current-induced damage decreases with increasing water depth. The wave-current load represented the decisive load case, with damage numbers of up to $S_{max} = 1.68$, which still do not meet the failure criteria defined by den Boon et al. (2004).

For the eroded beach configuration larger damage numbers have been measured for hydraulic offshore boundary conditions equal to the normal beach profile. This increased damage number is

attributed to a higher amount of wave energy (+10%) reaching the pile under the eroded beach configuration.

It was found that also the load history has an influence on the maximum damage number. The 1/100 year return period load conditions were tested at the eroded beach configuration for a sequence of three increasing flow velocities (blue diamonds, $U_c(\mathrm{m/s}) = 2.01, 2.22, 2.59$). This led to a continuous global erosion of the whole mobile test section, as each sequence lasted for 3500 waves. Then, the test was repeated with a fresh sand bed only for the highest flow velocity and the same wave conditions. The damage number reduced to a value of 70% compared to the sequential increased loading. It can be concluded that the period since the last nourishment at the monopile influences the resulting damage number.

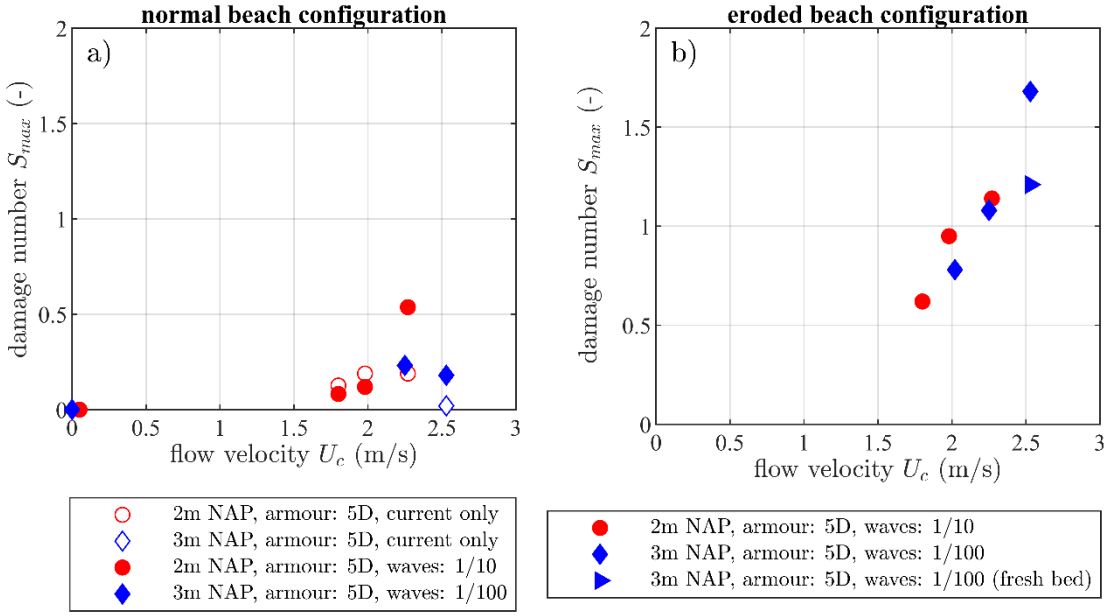

Figure 8. Derived damage numbers for the (a) normal and (b) eroded beach profile for current only conditions (hollow circles), wave and current loading for the 1/10 year return period (red circles) as well as the 1/100 year return period (blue diamonds).

DISCUSSION

In the model tests, the bottom filter layer (1-200 mm in prototype scale) was replaced by a geotextile for two reasons: (1) the damage assessment focused on displacement of armour stones from the top layer of the scour protection and (2) to prevent winnowing processes from affecting the results. It is expected that this decision leads to clearer detections of the erosion stability of the top armour layer. The sand in the model tests ($D_{n,50} = 0.17mm$) could not be scaled in accordance with the applied FROUDE scale as the grading would become too fine and starts to behave cohesive. Hence, the proportion of the diameter of the armour stones to the sand particles (D_{armour}/D_{sand}) is 35 times smaller than in prototype conditions. Some of the derived stability numbers show a bias from the expected trend. It is assumed that this bias is caused by the subjective placement of the individual filter layers and sand cover. The two analyzed wave conditions (1/10 and 1/100 year return period) show a constant wave steepness of 0.042. Hence, the derived correlations are only valid for relatively steep waves. The ripples in the mobile sand layer in this study are oversized compared to the prototype; a known model effect in scaled hydraulic models that is not to be circumvented.

CONCLUSIONS

To verify the stability of a conceptual scour protection design installed around monopiles in varying water depths ($0.047 < d/L_p < 0.057$) and under combined wave and current loads, physical model tests were conducted at a scale of 1:35 in a 3D wave-current basin at Ludwig-Franzius-Institute, Leibniz University Hannover. The tests had a unique boundary condition in that the scour protection was buried under a mobile sand bed. The scouring process of this sand layer was studied as well as the stability of the armour layer of the underlying scour protection.

The characteristics of the scour development and the deformation of the armour layer were determined for various wave-current load combinations. The deformation of the armour layer was

documented using 3D laser scans and analyzed with non-dimensional damage numbers, which enabled a comparison of the stability of the scour protection design. The main conclusion of this study is that the scour protection design is stable under the studied conditions.

Current-induced flow was the dominant factor for the scouring of the sand layer, with the scour development following known trends for steady current-induced scouring. In wave only condition, the scouring process was significantly slower and the hydraulic load was not sufficient to reach the embedded scour protection (for the normal beach profile). In current and combined wave-current condition, the further progression and expansion of the scour hole was obstructed after the scour protection layer was reached.

The scour hole tended to be asymmetrically, characterized by steeper slopes and a smaller extension from the pile at the upstream side of the pile (in current direction) compared to the down-stream side. Slopes and shape of the scour hole were similar to that found under unidirectional current, emphasizing the importance of the current flow for the scouring process.

For tests with an eroded beach profile, most of the scour protection was uncovered. In current and wave-current conditions, the level of scour protection movement reached from "rocking" of exposed stones to a clear albeit local deformation of the scour protection layer. The movement of individual stones from the scour protection increased with increasing current flow velocity, thinner sand cover and increasing water depth, which are boundary conditions inherent to the eroded beach profile.

ACKNOWLEDGMENTS

The presented hydraulic model tests have been initiated by Royal HaskoningDHV, The Netherlands, in order to assess the stability of a buried scour protection in shallow coastal waters. The advanced analysis of the data has benefited from additional funding from the German Research Foundation. (DFG, German Research Foundation) - SFB1463 - 434502799.

REFERENCES

CIRIA (2007). *The rock manual*. The use of rock in hydraulic engineering. CIRIA C683, London

Chavez CEA., Stratigaki V., Wu M., Troch P., Schendel A., Welzel M. et al. (2019). Large-scale experiments to improve monopile scour protection design adapted to climate change – the PROTEUS project. *Energies*, 12(9), 1709. https://doi.org/10.3390/en12091709.

Deltares (2016). Borssele OHVS – Scour and scour protection. Physical modelling test programme. Ref: 1230394-000-HYE-0011; report, dated October 2016.

De Vos, L., De Rouck, J., Troch, P., & Frigaard, P. (2012). Empirical design of scour protections around monopile foundations. Part 2: Dynamic approach. *Coastal Engineering*, 60, 286–298. https://doi.org/10.1016/j.coastaleng.2011.11.001.

Den Boon, H., Sutherland, J., Whitehouse, R., Soulsby, R., Stam, C.-J., Verhoeven, K., Høgedal, M., & Hald, T. (2004). Scour behaviour and scour protection for mono-pile foundations of offshore wind turbines. *European Wind Energy Conference & Exhibition EWEC*, 14.

Fazeres-Ferradosa, T., Welzel, M., Schendel, A., Baelus, L., Santos, P. R., & Pinto, F. T. (2020). Extended characterization of damage in rubble mound scour protections. *Coastal Engineering*, 158, 103671. https://doi.org/10.1016/j.coastaleng.2020.103671.

Qi, W.-G. and Gao, F.-P. (2014). Physical modelling of local scour development around a large-diameter monopile in combined waves and current. *Coastal Engineering* 83, pp. 72–81. DOI: 10.1016/j.coastaleng.2013.10.007.

Schendel A., Welzel M., Hildebrandt A., Schlurmann T., Hsu T-W. (2019). Role and impact of hydrograph shape on tidal current-induced scour in physical-modelling environments. *Water* (Switzerland), 11(12), 2636. https://doi.org/10.3390/w11122636.

Schendel, A.; Welzel, M.; Schlurmann, T.; Hsu, T.-W. (2020). Scour around a monopile induced by directionally spread irregular waves in combination with oblique currents. *Coastal Engineering* 161, 103751. DOI:10.1016/j.coastaleng.2020.103751.

Sumer, B. M., & Fredsøe, J. (2002). The mechanics of scour in the marine environment. Ed. by B. M. Sumer and J. Fredsøe. World Scientific - New Jersey - Singapore -London - Hong Kong.

Van der Meer, J. W. (1988). Rock slopes and gravel beaches under wave attack. *Dissertation, Technical University Delft*. https://www.elibrary.ru/item.asp?id=6844340.

WindEurope (2021). Offshore wind in Europe - Key trends and statistics 2020. *Tech. rep. WindEurope*.

Whitehouse, R. J. S. W. (1998). *Scour at marine structures: A manual for practical applications*. Thomas Telford Publications, London.